PREPARATION OF POROUS SILICON STRUCTURE EMBEDDED WITH CdS FOR H_2S Gas SENSING APPLICATIONS AND ITS INFLUENCE ON THE ENVIRONMENT

Raghad H. Mohsin[1] Hasan A. Hadi.[1] Raid A. Ismail*[2]
Researcher Prof. Prof.
[1]Department of Physics, College of Education, Mustansiriyah University, Baghdad, Iraq
[2]Department of Applied Science, University of Technology, Baghdad, Iraq
***Corresponding author: raghad_hamdan@uomustansiriyah.edu.iq**

ABSTRACT

This study aimed to prepare and characterize a gas sensor based on porous silicon embedded with CdS using the laser-assisted chemical bath deposition method. The structural and optical properties of CdS thin film prepared at deposition time of 30 min were studied by X-ray diffraction (XRD), scanning electron microscope (SEM), atomic force microscope (AFM), energy dispersive X-ray (EDX), and UV-Vis spectrophotometer. The (XRD) results showed that the deposited CdS film was crystalline and the crystallinity of the film improved after using laser during deposition of the film. The value of optical energy gap of the CdS film deposited without and with laser irradiation were found to be 2.5 eV and 2.68 eV, respectively. The gas sensor based on CdS-embedded porous silicon exhibit good sensitivity to H_2S gas. The sensor enables rapid detection of toxic H_2S gas, minimizing health and environmental risks and enhancing safety in industrial places.

Keywords; Thin film; Chemical bath deposition; gas sensor, environmental monitoring

مجلة العلوم الزراعية العراقية- 2025 :56 (4):1561-1573 محسن آخرون

تركيب سيليكون مسامي مدمج مع CdS لتطبيقات تحسس غاز H_2S وتأثيره في البيئة

رغد حمدان محسن حسن عبد الصاحب هادي رائد عبد الوهاب إسماعيل
باحثة استاذ استاذ
[1]قسم الفيزياء، كلية التربية، جامعة المستنصرية، بغداد، العراق
[2]قسم العلوم التطبيقية، جامعة التكنولوجيا، بغداد، العراق

المستخلص

هدفت الدراسة الى تحضير وتوصيف متحسس غاز من السيليكون المسامي المدمج بجسيمات نانوية CdS بأستعمال طريقة ترسيب الحمام الكيميائي بمساعدة الليزر. تم دراسة الخصائص التركيبية والبصرية لغشاء CdS الرقيق الذي تم تحضيره في وقت ترسيب قدره 30 دقيقة باستخدام حيود الأشعة السينية (XRD)، المجهر الإلكتروني الماسح (SEM)، مجهر القوة الذرية (AFM)، الأشعة السينية المشتتة للطاقة (EDX)، ومقياس الطيف الضوئي للأشعة فوق البنفسجية والمرئية (UV–Vis). تُظهر نتائج حيود الأشعة السينية(XRD) أن الغشاء المترسب من CdS كان بلوريًا وأن بلورية الغشاء تحسنت بعد أستعمال الليزر أثناء ترسيب الغشاء. تم العثور على قيمة فجوة الطاقة البصرية لغشاء CdS المترسب بدون ومع الإشعاع بالليزر لتكون 2.5 إلكترون فولت و2.68 إلكترون فولت، على التوالي. يظهر متحسس الغاز القائم على السيليكون المسامي المدمج مع CdS تحسس جيد لغاز H_2S، يساعد المتحسس في الكشف السريع عن غاز H_2S السام، مما يقلل من مخاطره على الصحة والبيئة ويعزز السلامة في الأماكن الصناعية.

الكلمات المفتاحية: غشاء رقيق,,ترسيب بطريقة الحمام الكيميائي, متحسس الغاز، مراقبة بيئية

Received:8 /12/2024, Accepted:2/2/2025, Published: August,2025

INTRODUCTION

In recent decades, growing industrialization and urbanization have led to sustained interest in the development of gas sensors for applications in environmental monitoring, agricultural, illness detection, home security, and automotive sectors (6, 31). Environmental pollution has become a critical concern due to the increase of industry and the growth of the human population (3). The four primary categories of environmental pollution are noise, water, air, and soil contamination. The pollution of air and water is detrimental not just to humans but also to the ecology (2, 3). Researchers have created several instruments, including gas sensors, air quality monitors, and water purifiers, to tackle these challenges and identify answers (3, 10, 29). The World Health Organization said that air pollution in 2012 was mostly caused by hazardous gases, leading to around 7.106 premature deaths [15, 17, 25). CdS films are n-type semiconductors with an energy gap around 2.4 eV at room temperature. It has two phases: cubic and hexagonal (34, 41). CdS films have been employed in many industrial and technological applications such as solar cells (8, 22, 23 28), transistors (36), gas sensors (7, 11, 33), light-emitting diodes (44), lasers (45), photocatalysts (17), biosensors (35), and biolabels (40). Many techniques were proposed to prepare CdS thin films like have chemical spray pyrolysis, electrochemical deposition, molecular beam deposition, laser ablation, chemical bath deposition, and SILAR approach (39,42). Porous silicon (PS) is an important semiconducting material and draw attention due to its unique chemical and physical properties. This structure exhibited excellent photoluminescence properties, tuned energy gap, high surface area, etc. These properties enable porous silicon used in many applications for example, gas sensors, photodetector, and light emitting (1,13, 14, 32). The porous silicon can be prepared by many methods such as anodization, laser-asssited electrochemical etching, and stain etching (4, 5, 24). For gas sensing application, the porous silicon as used effectively for sensing of NO_2 and H_2S (29). Embedded of porous silicon with thin films have attracted interest due to improvement of its characteristics via reduction in structural defects and forming additional heterostructure devices. Several data have been reported on embedded on nanoparticles in porous silicon (19, 38). In this regard, The main objective of this work is to fabricate CdS-embedded porous silicon sensor or H2S gas by laser-assisted chemical bath deposition and electrochemical etching. The structural and optical, and sensing properties ere investigated.

MATERIALS AND METHODS

All the chemical including cadmium chloride ($CdCl_2.H_2O$) provided by New Delhi, INDIA), thiourea (NH_2CSNH_2, quality 99% ,New Delhi, INDIA), and ammonia solution (NH_3) were used as provided without further purification or filtration for deposition of CdS.

Preparation of porous silicon

The porous silicon as prepared by electrochemical etching procedure. The silicon used was mirror-like p-type with orientation of (100) having 500 µm thickness and electrical resistivity of 10 Ωcm. The silicon substrate was cut into pieces with areas of 1 cm^2. The samples were sequentially cleaned using ultrasonic for five min using ethanol, acetone, and distilled water. After cleaning, the samples were drayed with heated air. The porous silicon was prepared using a home-made photo-electrochemical Teflon cell and the details of this cell are presented elsewhere (21). The PSi layer prepared with the aid of halogen lamp to produce current.. The samples are immersed in the cell filled with a mixture of alcohol and hydrofluoric acid HF with concentration of 48%. The current density and etching time were 10 mA/cm² and 10 minutes, respectively. This condition was selected precisely in order to produce a thin porous layer and low-porosity surface.

Deposition of CdS thin films

Glass and porous silicon substrates were coated with CdS thin films after 30 minutes. All of the trials were conducted with a constant put the salt in a 250 mL beaker with 100 mL of deionized water. Mix until dissolved entirely. 0.1 M of cadmium sulfate and 0.3 M of thiourea, respectively. A beaker with 100 milliliters of deionized (DI) water was used as the chemical bath system, which was continuously stirred at 90 degrees Celsius. The substrates used were glass slides

measuring 25 mm by 25 mm by 1 mm. We started by washing them in an ultrasonic bath with methanol, acetone, and deionized water (DI) for 15 minutes. After that, we dried them with hot air before using them as a substrate for the CdS thin film deposition process. In this investigation, p-type silicon with a (100) orientation and an electrical resistivity between 3 and 5 Ωcm was used. The silicon substrate had a surface area of one square centimeter. The substrates were cleaned using the RCA procedure before the film was deposited. A solution was made by mixing 5 milliliters of aqueous ammonia with cadmium sulfate in deionized (DI) water at room temperature in order to develop a CdS film. As a buffer, ammonium sulfate was added at 40°C. Before adding an additional 5 ml of aqueous ammonia, thiourea was added to the solution at 50°C. The ultimate volume of the solution was around 100 milliliters. The operation of the chemical bath was conducted at 90°C for 30 minutes of deposition time.

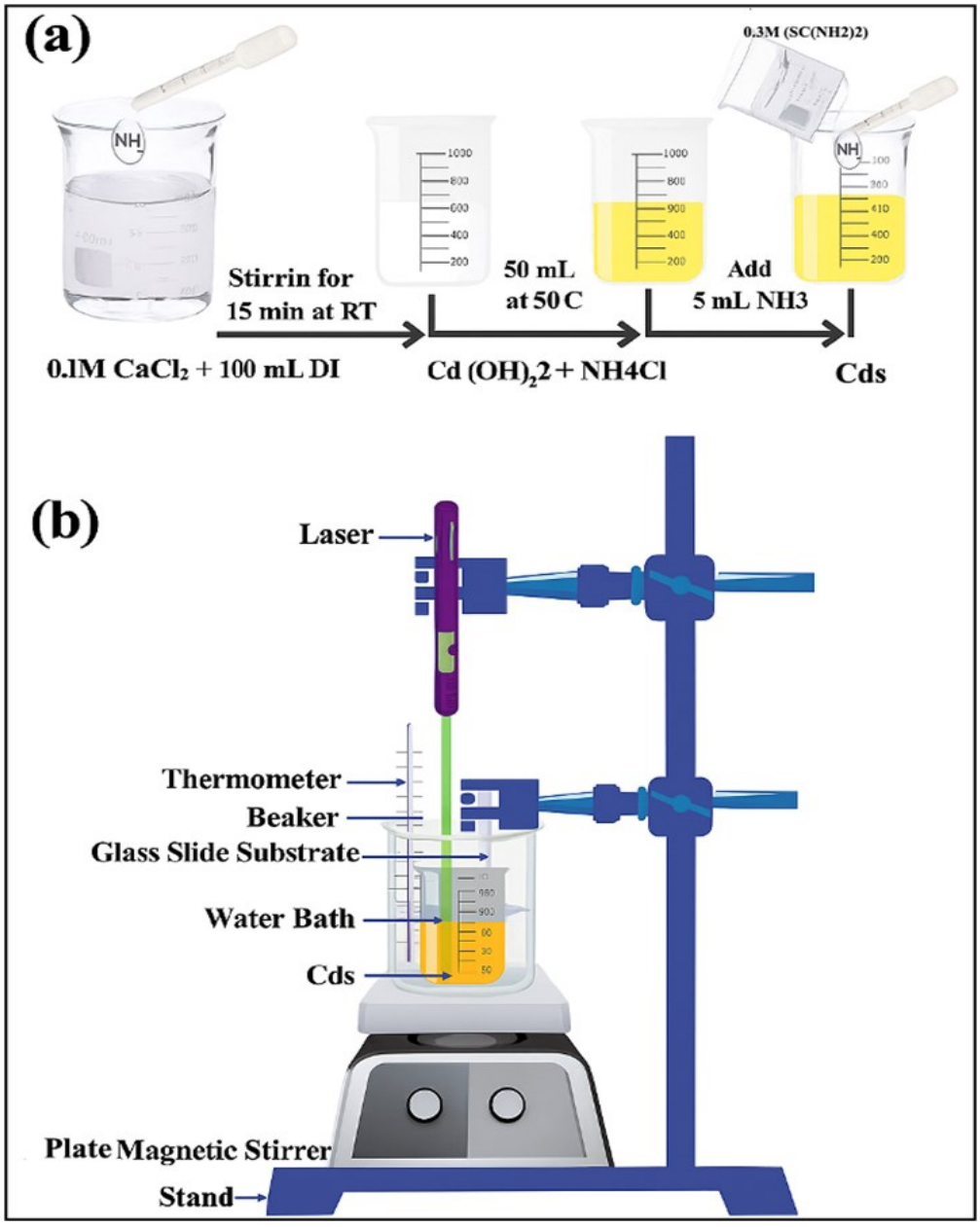

Figure 1. (a) preparation of CdS solution steps and (b) Systematic diagram of laser-assisted-chemical bath deposition system

in as shown in Fig. (1.a,b).

Characteristics: The structural properties of the porous silicon and CdS film were investigated using X-ray diffractometer (AERIS- XRD from PANalytical) using Cu-Kα radiation with λ = 0.15406 nm . The topography of the of the film as studied atomic force microscope (AFM model). The

morphology of the porous silicon and CdS film as investigated by field emission scanning electron microscopy FESEM (Inspect f 50-FEI business) and the chemical composition was estimated using energy dispersive X-ray EDX. UV-VIS spectrophotometer (Jasco V670/Japan) was employed to measure the optical properties of the CdS films deposited on glass substrate. Raman Microscope setup (Bruker Sentera Germany) using a 532 and 58nm laser wavelength.

RESULTS AND DISCUSSION

Structural properties: The CdS film XRD patterns on glass substrates prepared with and without laser irradiation are shown in Figure 2. Every film has crystalline structures, as can be seen, and the laser affects how crystallinity occurs. This figure confirms the formation of a polycrystalline CdS with a cubic structure. The 26.74° and 32.43° prevailing growth directions are (111) and (200) planes, respectively. The results are somewhat consistent with the international standards for the CdS phase with a cubic structure (reference code: 00-001-0647). (26). The grin size varies from 2.592nm at 30 min.. The results of the study reveal the size of the Cds nanocrystallites increase is essentially influence by using the laser. The dependence on laser effects can be related to accumulation and a more intensity and uniformity comparison during the deposition time without laser. Using the Scherrer formula , the average grain size (L) was determined for each film made for the preferred direction and it was discovered that, as indicated in Table (1) .In crystalline materials, the size of the grain has a significant impact on the material's characteristics by using eq.1 (19):

$$L = \frac{0.9\ \lambda}{\beta\ COS\theta} \qquad (1)$$

Where λ is the x-ray wavelength, β is half the peak width, and θ is the peak angle. The density of dislocation of thin films is calculated using the following formula (17). The study used Eqs.

2 and 3 to calculate dislocation density and grain count per unit area, finding that as particle size increases, the density of dislocations and grain count decrease

$$\delta = \frac{1}{L^2} \qquad (2)$$

-and The Cds microstrain (ε) could be calculated (43).

$$\varepsilon = \frac{FWHM \times \cot\theta}{4} \qquad (3)$$

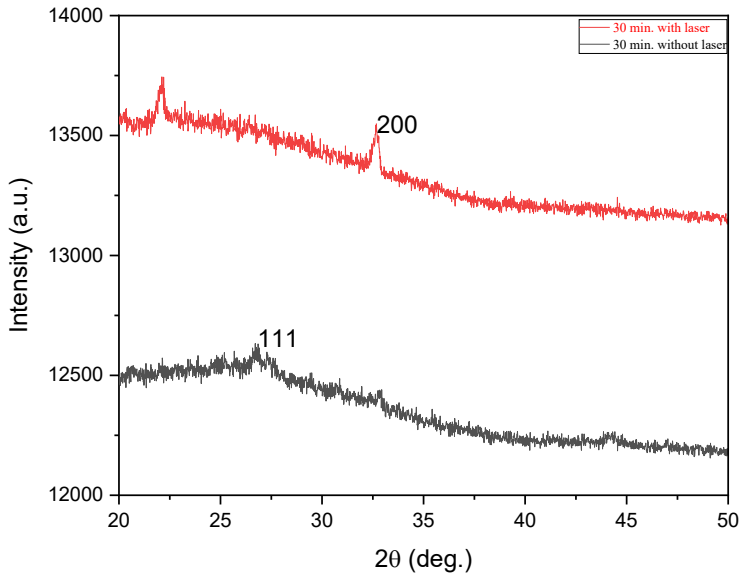

Figure 2. XRD pattern of Cds thin films preparation by CBD at deposition time 30 min before and after exposure to green laser

The deposition time in the chemical deposition process with laser assist has a significant effect on the structural properties of cadmium sulfide (Cds) layers. In general, time affects the crystal size, crystal distortion, layer thickness, and surface morphology.

Table 1. Effect of deposition time without laser and with laser on the Structural parameters of Cds thin films

Deposition Time (min)	Laser Effect	2θ (Deg.)	FWHM (Deg.)	d_{hkl} (Å)	L (nm)	Hkl	Lattice constant (Å)	$\delta \times 10^{15}$ $(\frac{lines}{m^2})$	ε $\times 10^{-3}$
30	Without laser	26.74	3.1495	3.3064	2.592	111	5.726	148.767	57.818
30	With laser	32.43	1.3809	2.7578	5.991	200	5.515	27.858	20.071

Morphological properties

AFM: To investigate the effect of the green laser on the surface properties of prepared Cds thin films prepared by chemical bath deposition (CBD) technique, atomic force microscopy (AFM) was employed. Fig. (3) illustrate the 3D, 2D, and histogram of average grain size distribution for CdS prepared with and without laser irradiation. The 3D AFM image confirms the formation of uniform CdS film with presence of some elongated CdS grains observed on the film surface for film deposited without laser. While the 3D image of the film deposited with laser shows the formation of more uniform CdS film with less elongated grains. This result indicates that these grain formed lastly which consisted of agglomerated grains. The root mean square of the surface roughness of CdS film with and without laser irradiation are listed in Table (2). This table shows that the square mean root (RMS) of CdS film prepared without and with laser irradiation was 3.264 and 1.993 nm, respectively. This result confirms the laser irradiation resulted in formation of smoother CdS film. The grain size distribution exhibits Gaussian –like distribution, since the distribution was found to be narrower for sample deposited with using laser.

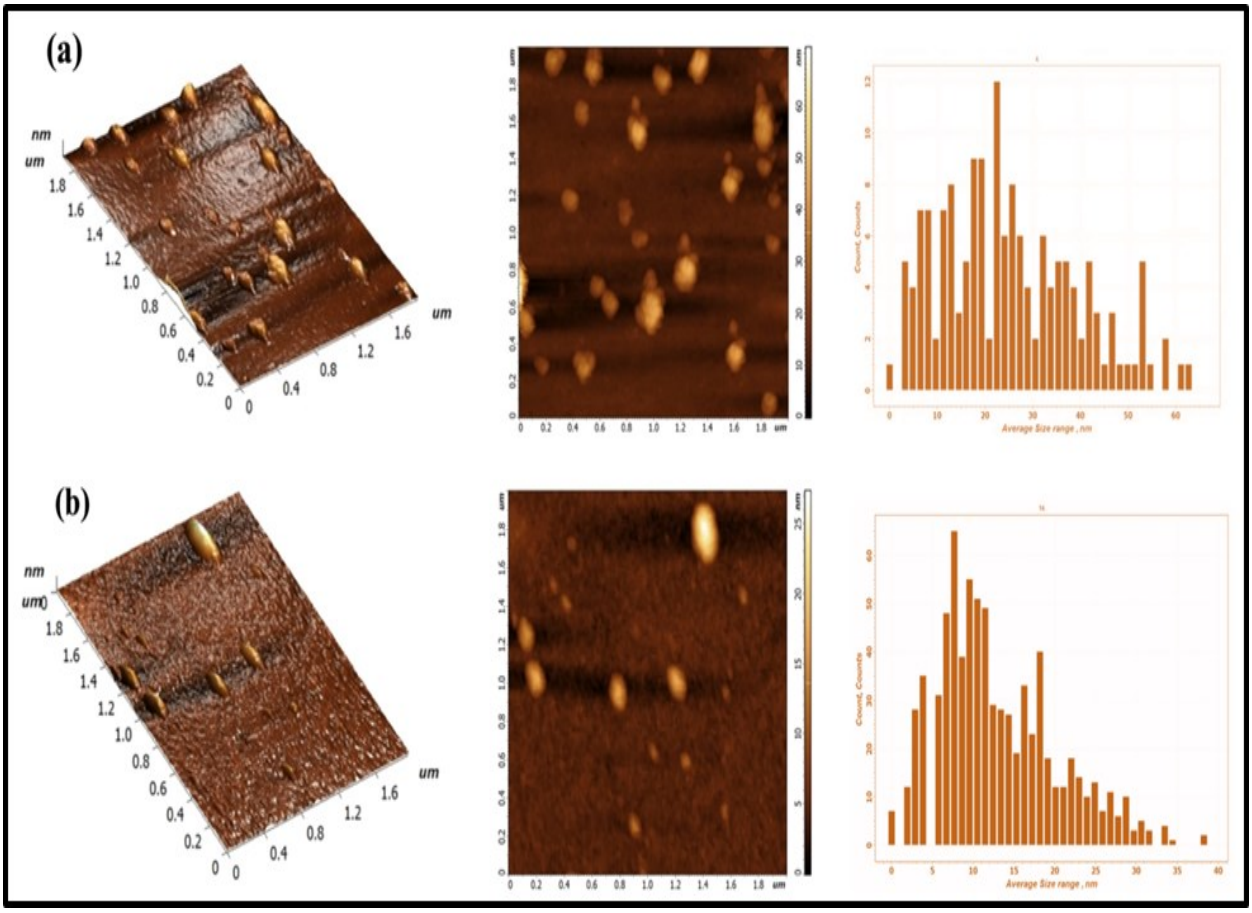

Figure 3. 3D, 2Dimages and grain size distribution of Cds prepared (a) without laser and (b) with laser

Table 2. Effect of deposition time without laser and with laser on the topographic layer of Cds

Sample	Time dop. (min)	RMS (nm)	Roughness average Sa (nm)	Peak-to-peak Sz (nm)
S1	30	3.264	5.957	71.163
S2	30 with laser	1.993	0.926	27.301

Figures (4) show the top view FE-SEM images of CdS prepared without and with laser and the insets are the cross section FESEM images of CdS. Fig.4a shows that the CdS film consisting of nanograins with average grain size of 70 nm.. The deposited CdS films are free of cracks and holes. The film deposited in presence of laser irradiation shows a significant improvement in the morphology, since the grains are spherical and almost have the same size which indicating the improvement in crystallinity quality. This result is consistent with XRD results. The cross section FESEM of CdS film shows the film was not uniform distributed on the substrate, while it was observed more uniform when the laser used during deposition. This is due to the laser is coherence beam and provide the grains power that helps them to reordering and formed high degree of crystallinity film.

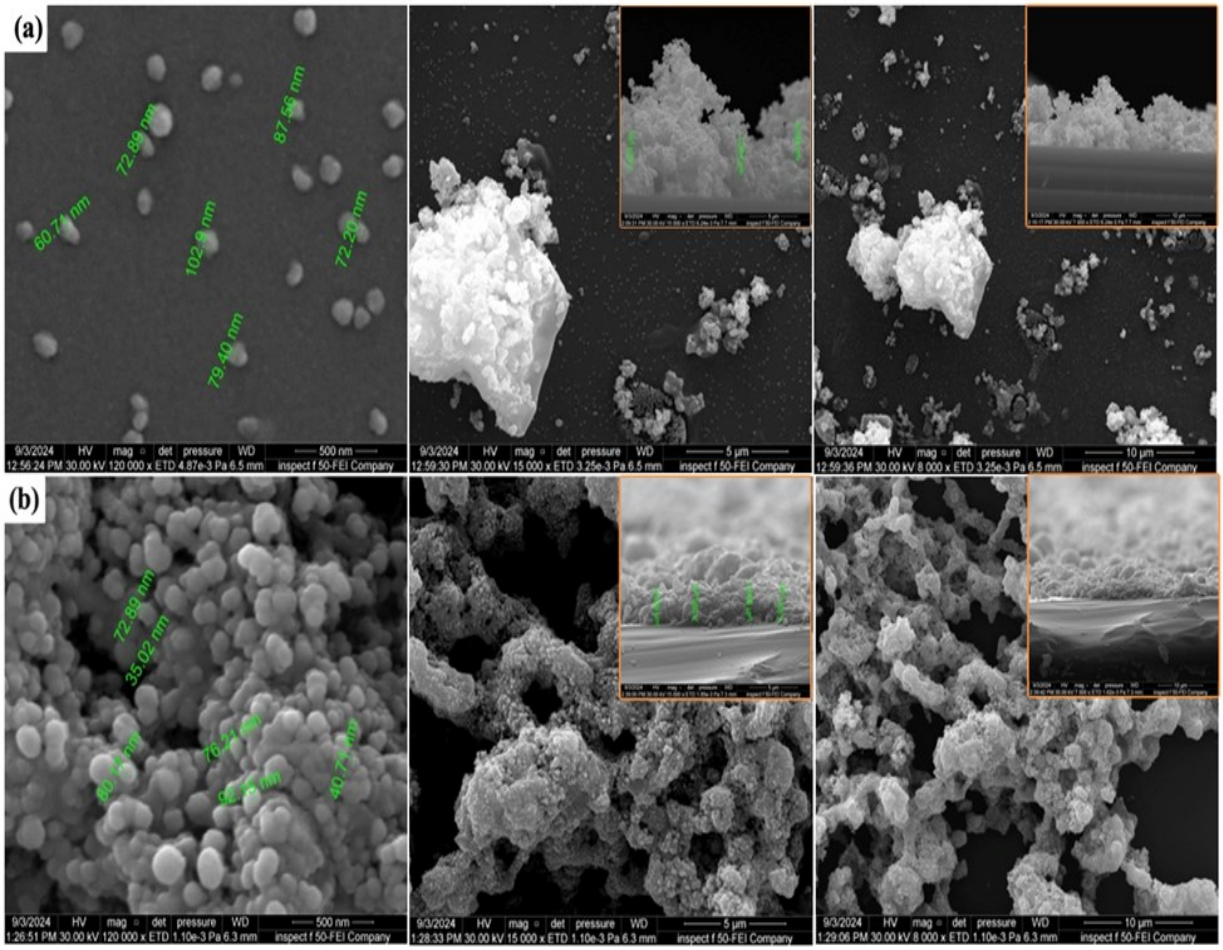

Figure 4. FESEM images with different magnifications of CdS film deposited on glass substrate prepared (a) without and (b) with laser. Insets are the cross section FESEM images

The FESEM image of CdS-embedded porous silicon are shown in Fig.(5). It is obvious from Fig.(5) that the CdS particles are filled the pores and distributed over the entire surface of the porous. We can see some agglomerated CdS particles on the surface which indicates that the pores are filled and the excess of CdS particles are formed on the surface. Fig.5b illustrates the creoss section FESEM image of CdS-porous silicon interface.

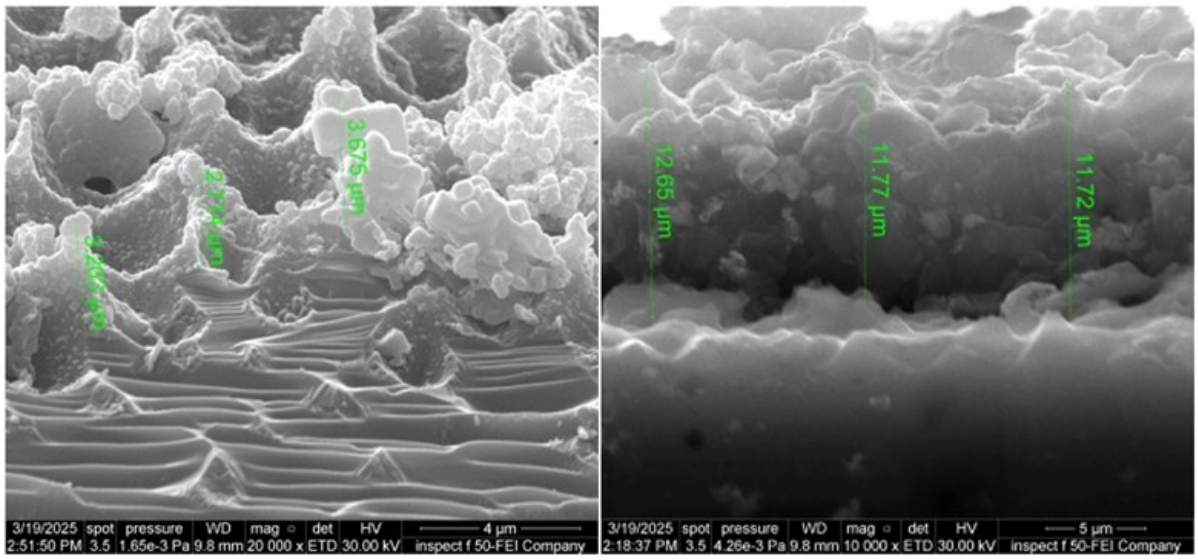

-a- -b-

Figure 5. FESEM of CdS film-embedded porous silicon (a) top view and (b) cross section of CdS-porous silicon

Fig.(6) illustrates the UV-VIS transmission plot of CdS film deposited on glass substrate without and with presence of laser beam. The transmittance were recorded in the range from 300 to 900nm. Enhanced crystallinity arisen from using laser beam results in increases the transmission of the CdS film. The main reason could be ascribed to crystallinity and decreasing the surface roughness. Decreasing the surface roughness of the film can contribute effectively in increasing the film's [5]transmission.

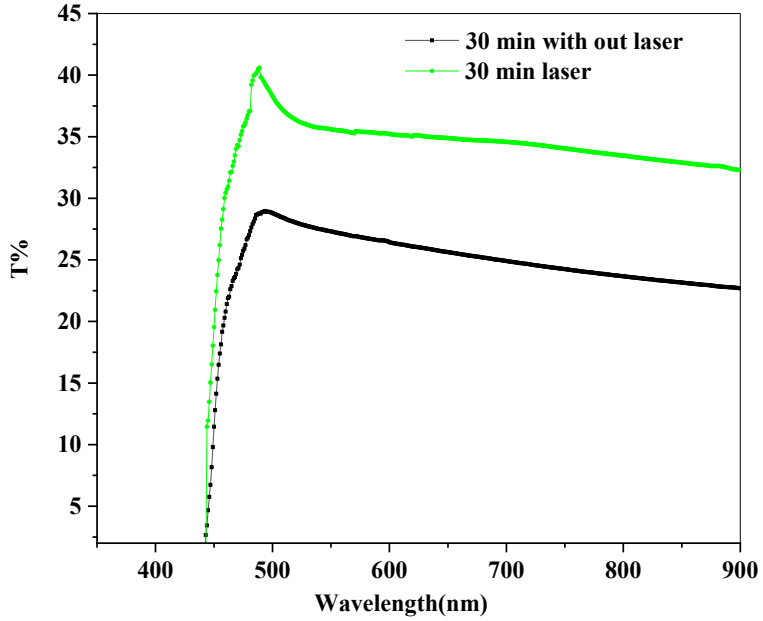

Figure 6. UV-VIS optical transmission spectra of the CdS thin films deposited without and with laser beam irradiation.

The optical energy gap (E_g) of CdS thin film for direct transitions was determined using equation Tauc method (37):

$$(\alpha h\nu)^n = A(h\nu - E_g) \quad (4)$$

where A is a constant, n is the exponent that determine the transition type, α refer to the absorption coefficient which can be calculated from the following relationship (30):

$$\alpha = \frac{1}{t} \ln \frac{1}{T} \quad (5)$$

where T is the transmittance in the high absorption region and t is the film thickness For direct transition, as in the case of CdS, the value of n = 1/2. A plot of $(\alpha h\nu)^2$ vs. $h\nu$ is shows in Fig. (8), the extrapolation of the linear part to photon energy axis gives the

value of optical energy gap (7), which is found Eg = 2.6 and 2.68 eV for films deposited without and with laser irradiation, respectively. These values are larger than the that of bulk CdS (Eg = 2.42 eV) due to the quantum size effect. The increase of optical energy gap with presence of the laser may be due to decreasing the grain size and improvement in film's (1) stoichiometry show Fig.7.

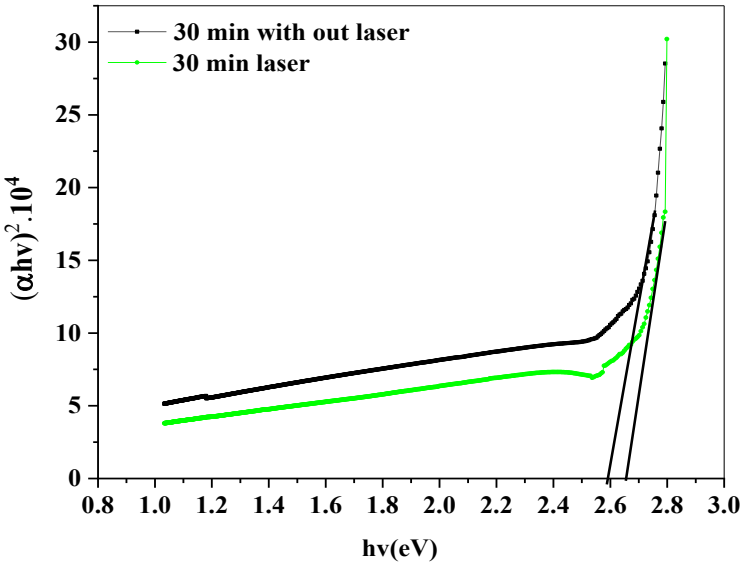

Fig 7. Variation of $(\alpha h\nu)^2$ with photon energy of CdS films deposited without and with laser beam

The elemental composition of the CdS films as determined by EDX. Fig. (8) shows the EDX spectra of CdS film deposited without and with laser. The spectra confirms the presence of main elements of the film: Cd and S. The weight percentage of Cd and S for film deposited with laser are 50.90 and 21.67, respectively, while the weight percentage of Cd and S without laser were 36.76 and 16.05, respectively. This result confirms that the stoichiometry of the film deposited with laser has improved and its (Cd)/(S) ratio is around 2.348. The EDX of Cds thin film show that the film contains amount N, O, Na, Si and Cl, these elements result from the solutions used in the chemical reaction in the preparation method and the initial nature of the glass substrate. From the EDX analysis of Cds nanoparticles prepared using the present technique are free from impurities is well understood ,the atomic proportion of Cd, S increased, by increasing the radiation from lasers and deposition time.

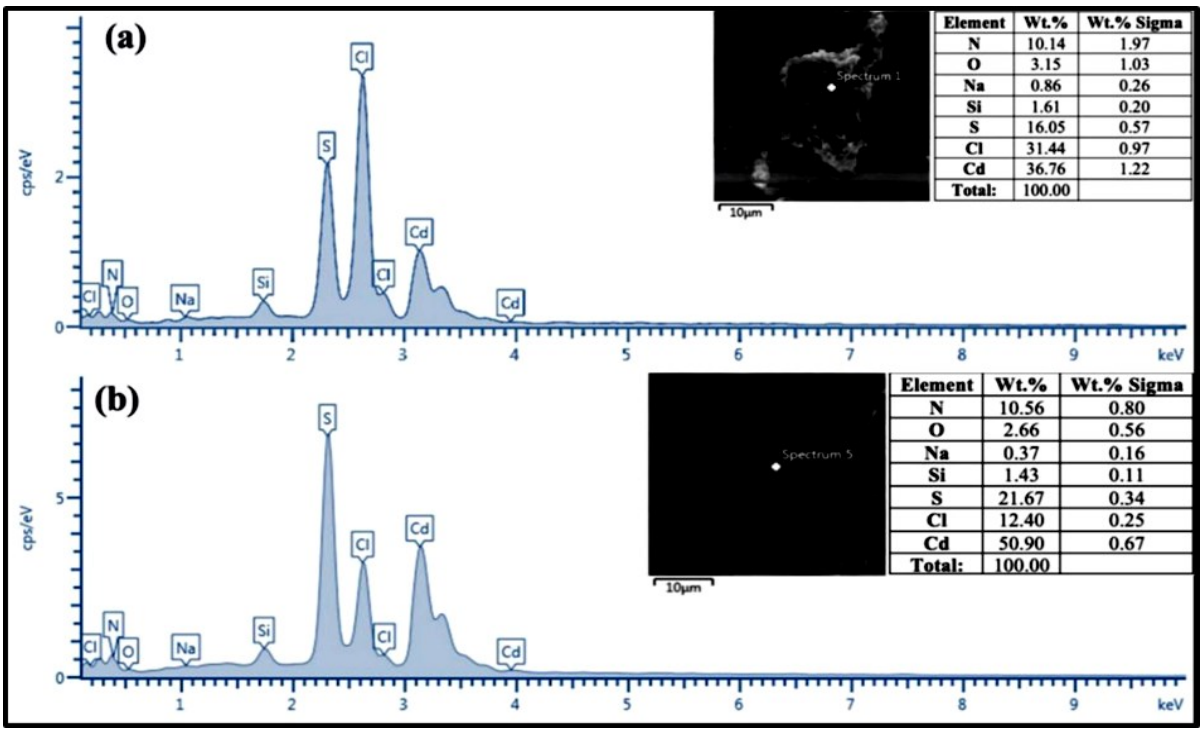

Figure 8. EDX spectra of CdS deposited (a) without and (bwith green laser

The Raman spectra of CdS films are shown in Fig. (9). These peaks could be identified as-multi-overtones of LO phonons, which contains 1LO (the first order), 2LO (the second order) and 3LO (third order), respectively at 300, 600 and 900 cm^{-1} which are consistent with reported results [9]. It can be observed that the intensity of Raman peaks is increased when the laser beam used during the deposition of the film. Indicating the improvement in film crystallinity.

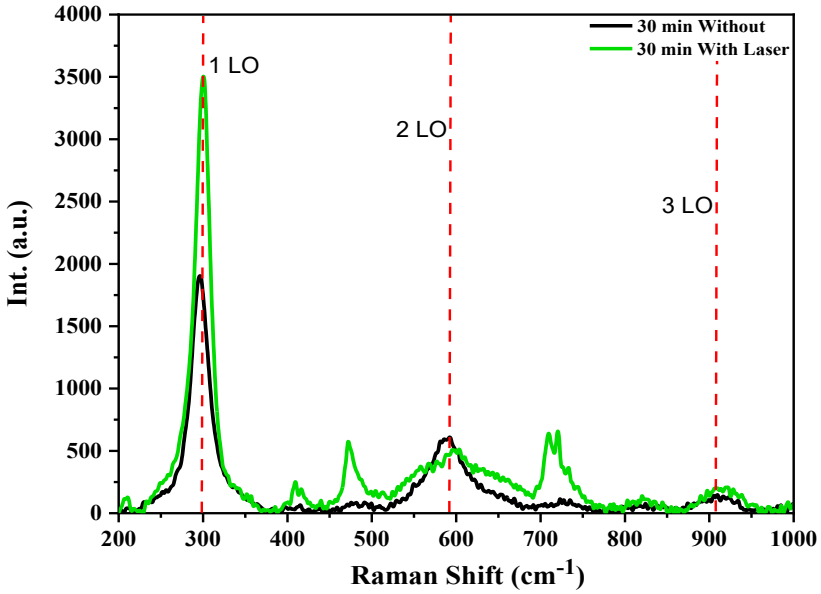

Figure 9. Raman spectra of CdS thin films

The gas sensing device was fabricated by depositing CdS film on porous silicon with and without laser. The sensing performance of the CdS-embedded porous silicon was investigated at 60 ppm concentration at different values of substrate temperatures: 75 °C,125 °C, and 175 °C. The variation of electrical resistivity with time plots when it exposure with H_2S gas are shown in Fig.(10). The electrical resistance increases when exposed to gas indicating the sensor has responded to the gas. Increases the electrical resistance after exposure to gas is due to adsorbed the H_2S gas atoms on CdS particles and after the gas is removed, the resistance returns to its original value. The stability and

repeatability of the sensors, with two nearly identical sensing cycles. The samples show stable and repeatable behavior for two dynamic responses, indicating the sensor's efficiency and stability. Fig.(10b) confirm that the sensitivity of the gas sensor was significantly increased when the laser used during the deposition of the CdS film. This improvement can be ascribed to reduction in structural defects accompanied the deposition of the films as well as the reduction in particles agglomeration [45].

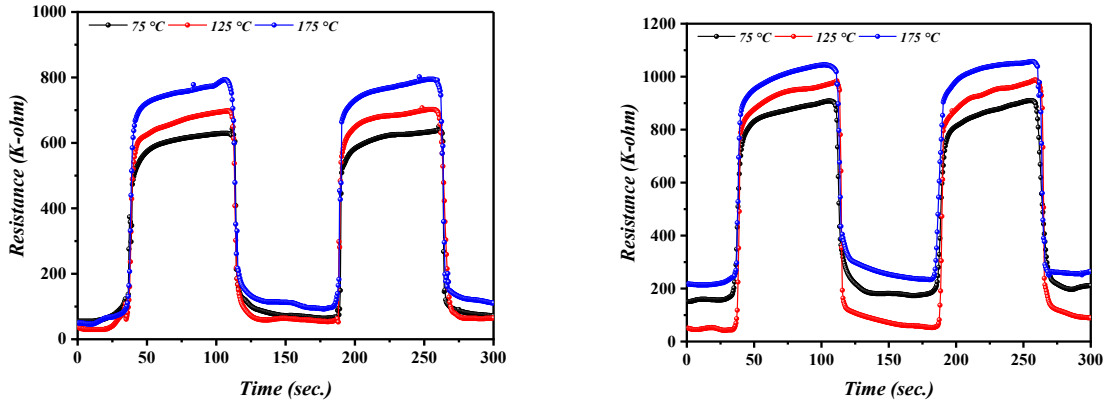

Figure 10. The resistance-time variation during exposure to H_2S gas for CdS-embedded porous silicon sensor at different temperatures (a) without using laser and (b) with laser

The sensitivity (S) is known as the ratio of $R_g - R_a$ to R_a, where R_g is the resistance in the presence of gas, and R_a is the electrical resistance in the air. The sensitivity of the samples was calculated by the following equation, with 75°C, 125 °C, 175 °C and 60 ppm [27].

$$S = \frac{R_g - R_a}{R_a} \times 100 \ldots\ldots\ldots (6)$$

The obtained results indicated that the laser affects the gas sensing properties of the sensor. It shows that sensitivity increases with both the presence of a laser and higher H_2S concentration. Furthermore, Table (3) includes that data of sensitivity, rise time, and recovery time, comparing the sample prepared without laser and with laser effect. The results suggest that laser presence improves response behavior, enabling more effective and reliable detection of H_2S at room temperature.

Table 3. lists the sensitivity, rise time, and recovery time of CdS-embedded porous silicon as sensors fabricated with and without laser

Samples	Sensitivity %					Rise time (s)			Recover time (s)		
	60 ppm			90 ppm	120 ppm	60 ppm			60 ppm		
	75 °C	125 °C	175 °C	75 °C	75 °C	75 °C	125 °C	175 °C	75 °C	125 °C	175 °C
Without laser	4.68	19.26	3.60	9.59	19.26	10.5	7.6	7	5.3	4.7	3.9
With laser	9.90	20.8	14.9	10.1	20.8	9.7	8	9.5	8.5	2.4	7.2

Conclusion

Cadmium sulfide (Cds) thin film has been synthesis by laser-assisted-chemical bath deposition (CBD) system. The structural, topographical, morphological, optical, and chemical properties of CdS were analyzed. The use of lasers during chemical deposition enhances crystal structure, reduces surface defects, and improves surface and morphological properties in CdS films, producing spherical grains with better crystallinity quality and aligning with XRD findings. Morphological investigation revealed that CdS particles were present in clusters on the porous silicon surface and inside the pore. The optical energy gap in films deposited without and with laser irradiation is larger than bulk CdS due to the quantum size effect and improved stoichiometry. A gas sensing device was created by depositing a CdS film on porous silicon with or without a laser. The sensor's performance was tested at different substrate temperatures and exposure to H_2S gas. The sensor's efficiency and stability were

confirmed, with a significant increase in sensitivity due to laser deposition and particle agglomeration. Improved surface and morphological characteristics contributed to the sensor's increased ability to detect H_2S gas. A sensor made with a laser effect exhibited reliable detection of H_2S at room temperature, and that can be applied in environmental or industrial contexts. This results make it possible to extend to other gases to test the efficiency of the multi-purpose sensor.

CONFLICT OF INTEREST

The authors declare that they have no conflicts of interest.

DECLARATION OF FUND

The authors declare that they have not received a fund.

REFERENCES

1. Ahmed, F. M., A. M. Muhammed Ali, I R. A. smail, M. A. Fakhri, and E. T. Salim, 2023. Investigating the influence of deposition time on nanostructured CdS film prepared by chemical bath deposition for photodetection applications. Journal of Materials Science: Materials in Electronics, 34(27), 1906. https://doi.org/10.1007/s10854-023-11380-z

2. Al-Janabi , Z. Z., F. M. Hassan, and A. H. M. J. Al-Obaidy, 2024. Overall index of pollution (oip) for tigris river, baghdad city, Iraq, Iraqi Journal of Agricultural Sciences, 55. (2) 905-916. https://doi.org/10.36103/gqq14f43

3. Alsaadoon, D. W. K., F. M. Hassan and W. M. Mahdi 2023. Assessement of water quality of diyala river using overall index of pollution (oip) in iraq. Iraqi Journal of Agricultural Sciences 54(3):682-690. https://doi.org/10.36103/ijas.v54i3.1748

4. Azaiez, K., R. B. Zaghouani, M. Daoudi, M. Amlouk, and W. Dimassi, 2021. Enhanced photoluminescence property of porous silicon treated with bismuth (III). Inorganic Chemistry Communications, 130, 108-679. DOI:https://doi.org/10.1016/j.inoche.2021.108679

5. Azaiez, K., R. B. Zaghouani, S. Khamlich, H. Meddeb, and W. Dimassi, 2018. Enhancement of porous silicon photoluminescence property by lithium chloride treatment. Applied Surface Science, 441, 272-276. https://doi.org/10.1016/j.apsusc.2018.02.006

6. Chatterjee, S. G., S. Chatterjee, A. K. Ray, and A. K. Chakraborty, 2015. Graphene–metal oxide nanohybrids for toxic gas sensor: A review. Sensors and Actuators B: Chemical, 221, 1170-1181. DOI: https://doi.org/10.1016/j.snb.2015.07.070

7. Du, N., Zhang, H., B. Chen, J. Wu, and D. Yang, 2007. Low-temperature chemical solution route for ZnO based sulfide coaxial nanocables: generalsynthesis and gas sensor application. Nanotechnology, 18(11), 115619. DOI 10.1088/0957-4484/18/11/115619

8. Dolai, S., R. Dey, S. Hussain, R. Bhar, and A. K. Pal, 2019. Photovoltaic properties of F: SnO2/CdS/CuO/Ag heterojunction solar cell. Materials Research Bulletin, 109: 1-9. DOI: https://doi.org/10.1016/j.materresbull.2018.09.022

9. Eman M. Noori and J. Nanostruct Winter, 2024, Properties of CdS Thin Films Prepared by Thermal Evaporation,14(1): 12-19, DOI: 10.22052/JNS.2024.01.002

10. Fine, G. F., L. M. Cavanagh, A. Afonja, and R. Binions, 2010. Metal oxide semi-conductor gas sensors in environmental monitoring. sensors, 10(6), DOI: 5469-5502. https://doi.org/10.3390/s100605469

11. Gao, N., and F. Guo, 2006. A hydrothermal approach to flake-shaped CdS single crystals. Materials Letters, 60(29-30), 3697-3700. https://doi.org/10.1016/j.matlet.2006.03.091

12. Gosavi, S. R., C.P. Nikam, A.R. Shelke, A.M. Patil, S.-W. Ryu, J.S. Bhat, and N.G. Deshpande, 2015. Chemical synthesis of porous web- structured CdS thin flms for photosensor applications. Mater. Chem. Phys. 160 , 244–250.DOI: https://doi.org/10.1016/j.matchemphys.2015.04.031

13. Hadi, H. A. 2014. Fabrication, morphological and optoelectronic properties of antimony on porous silicon as MSM photodetector. Journal of Fundamental and Applied Sciences 6.2: 175-186. DOI: 10.4314/jfas.v6i2.4

14.Hasan A. Hadi · Sarab T. Kasim · Fadhil K. Farhan·Raid A. Ismail·and N. F. Habubi 2023. Effect of Porosity on Thermal Properties of

Porous Silicon, Silicon 15.6: 2715-2725 DOI: https://doi.org/10.1007/s12633-022-02185-6)
15.Hermawan, A., N. L. W. Septiani, A. Taufik, B. Yuliarto, Suyatman, and S. Yin, 2021. Advanced strategies to improve performances of molybdenum-based gas sensors. Nano-Micro Letters, 13, 1-46. https://doi.org/10.36103/2twexb46
16. Ismail, R. A., K. S. Khashan, and A.M. Alwan, 2017. Study of the Effect of Incorporation of CdS Nanoparticles on the Porous Silicon Photodetector. Silicon 9, 321–326. DOI: https://doi.org/10.1007/s12633-016-9446-4
17. Ji, H., Zeng, W., and Y. Li, 2019. Gas sensing mechanisms of metal oxide semiconductors: a focus review. Nanoscale, 11(47), 22664-22684. DOI https://doi.org/10.1039/C9NR07699A
18. Kavil, J., A. Alshahrie, and P. Periyat, 2018. CdS sensitized TiO2 nano heterostructures as sunlight driven photocatalyst. Nano- Structures & Nano-Objects, 16, 24-30. https://doi.org/10.1016/j.nanoso.2018.03.011
19. Kazeminezhad, I., N. Hekmat, and A. Kiasat, 2014. Effect of growth parameters on structural and optical properties of CdS nanowires prepared by polymer controlled solvothermal route. Fibers and Polymers, 15, 672-679. DOI: https://doi.org/10.1007/s12221-014-0672-3
20. Lisco, F., P. M. Kaminski, A. Abbas, K. Bass, J. W. Bowers, G. Claudio, and J. M Walls,. 2015. The structural properties of CdS deposited by chemical bath deposition and pulsed direct current magnetron sputtering. Thin solid films, 582, 323-327. https://doi.org/10.1016/j.tsf.2014.11.062
21. Lu, C., L. Zhang, Y. Zhang, S. Liu, and G. Liu, 2014. Fabrication of CdS/CdSe bilayer thin films by chemical bath deposition and electrodeposition, and their photoelectrochemical properties. Applied surface science, 319, 278-284. https://doi.org/10.1016/j.apsusc.2014.08.158
22. Majumder, S., A. C. Mendhe, and B. R. Sankapal, 2019. Nanoheterojunction through PbS nanoparticles anchored CdS nanowires towards solar cell application. international journal of hydrogen energy, 44(14), 7095-7107. https://doi.org/10.1016/j.ijhydene.2019.01.277
23. Mathew, X., J. P. Enriquez, A. Romeo, and A. N. Tiwari, 2004. CdTe/CdS solar cells on flexible substrates. Solar energy, 77(6), 831-838. https://doi.org/10.1016/j.solener.2004.06.020
24. Mhamdi, H., R. B. Zaghouani, Fiorido, T., J. L. Lazzari, M. Bendahan, and W. Dimassi, 2020. Study of n-WO 3/p-porous silicon structures for gas-sensing applications. Journal of Materials Science: Materials in Electronics, 31, 7862-7870. DOI: https://doi.org/10.1007/s10854-020-03324-8
25. Mirzaei, A., J. H. Lee, S. M. Majhi, M. Weber, M. Bechelany, H. W. Kim, and S. S. Kim, 2019. Resistive gas sensors based on metal-oxide nanowires. Journal of Applied Physics, 126(24).DOI: https://doi.org/10.1063/1.5118805
26. Nan, Y. X., F. Chen, L. G. Yang, and H. Z. Chen, 2010. Electrochemical synthesis and charge transport properties of CdS nanocrystalline thin films with a conifer-like structure. The Journal of Physical Chemistry C, 114(27), 11911-11917. DOI: https://doi.org/10.1021/jp103085n
27. Hayif, N. D., H. A. Hadi, and I. H. Hashim, 2025. Enhancing the gas sensing of porous silicon by surface modification using non-thermal plasma. Journal of Materials Science: Materials in Electronics, 36(13), 806. 36):806. https://doi.org/10.1007/s10854-025-14867-z
28. Parasuraman, K., and P. Samiyammal et al. 2019. Improved magnetic and photocatalytic properties of spray deposited (Li+Co) codoped CdS thin films Superlattice. Microst. 129, : 28-39.DOI: https://doi.org/10.1016/j.spmi.2019.03.005
29. Perillo, P.M., and D.F. Rodriguez, 2024. CdS thin film sensor for NO_2 and H_2S detection at room temperature. Appl. Phys. A 130, 372. https://doi.org/10.1007/s00339-024-07545-0
30. Qian, H., Z., Liu, J. Ya, Y. Xin, J. Ma, and X. Wu, 2021. Construction homojunction and co-catalyst in ZnIn2S4 photoelectrode by Co ion doping for efficient photoelectrochemical water splitting. Journal of Alloys and Compounds, 867, 159028.

DOI:
https://doi.org/10.1016/j.jallcom.2021.159028
31. Rai, P., S. Raj, K. J. Ko, K. K. Park, and Y. T. Yu, 2013. Synthesis of flower-like ZnO microstructures for gas sensor applications. Sensors and Actuators B: Chemical, 178, 107-112 .
DOI:
https://doi.org/10.1016/j.snb.2012.12.031
32. Raid A. I.., 2010. Fabrication and Characterization of Photodetector Based on Porous Silicon. e-Journal of surface Science and Nanotechnology 8: 388-391.
DOI: https://doi.org/10.1380/ejssnt.2010.388
33. Ratinac, K. R., W. Yang, S. P. Ringer, and F. Braet, 2010. Toward Ubiquitous Environmental Gas Sensors Capitalizing on the Promise of Graphene. Environmental science & technology, 44(4), 1167-1176. https://doi.org/10.1021/es902659d
34. Ramadan, M., M. S. Elnouby, O. El-Shazly, E. F. El-Wahidy, A. A. M. Farag, and N. Roushdy, 2022. Facile fabrication, structural and electrical investigations of cadmium sulfide nanoparticles for fuel cell performance. Materials for Renewable and Sustainable Energy, 11(3), 277-286.
DOI: https://doi.org/10.1007/s40243-022-00220-5
35. Rathinamala, I., N. Jeyakumaran, and N. Prithivikumaran, 2019. Sol-gel assisted spin coated CdS/PS electrode based glucose biosensor. Vacuum, 161, 291-296.
https://doi.org/10.1016/j.vacuum.2018.12.045
36. Saha, U., and M. K. Alam, 2019. A hete rojunction bipolar transistor architecture-based solar cell using CBTSSe/CdS/ACZTSe materials. Solar Energy, 184, 664-671. DOI: https://doi.org/10.1016/j.solener.2019.04.044
37. Samiyammal, P., K. Parasuraman, and A. R. Balu, 2019. Improved magnetic and photocatalytic properties of spray deposited (Li+Co) codoped CdS thin films. Superlattices and Microstructures, 129, 28-39.
DOI:
https://doi.org/10.1016/j.spmi.2019.03.005
38. smail, R. A., S. A. Huseen, and T. D. Abass, 2025. Preparation of High-performance $BaTiO_3$ Nanoparticles-embedded Porous Silicon Photodetectors by Electro-chemical Etching and Laser Ablation in Liquid. Silicon 17, 205–218.
DOI:
https://doi.org/10.1007/s12633-024-03194-3.
39. Smt Swapna S., M. S Shinde, and R. S. Patil. 2016. Synthesis and Characterization of Cadmium Selenide Nanocrystalline Thin Films Prepared Using Novel Chemical Approach. J. Nano. Adv. Mat.; 4(2): 53-57.
DOI: http://dx.doi.org/10.18576/jnam/040202
40. Tabrizi, M. A., Ferré-Borrull, J., Kapruwan, P., and L. F. Marsal, 2019. A photoelectrochemical sandwich immunoassay for protein S 100β, a biomarker for Alzheimer's disease, using an ITO electrode modified with a reduced graphene oxide-gold conjugate and CdS-labeled secondary antibody. Microchimica Acta, 186, 1-9.
DOI: https://doi.org/10.1007/s00604-018-3159-x
41. Waldiya, M., R. Narasimman, D. Bhagat, D. Vankhade, and I. Mukhopadhyay, 2019. Nanoparticulate CdS 2D array by chemical bath deposition: Characterization and optoelectronic study. Materials Chemistry and Physics, 226, 26-33.
https://doi.org/10.1016/j.matchemphys.2019.01.017
42. Yadav, A. A, M. A., Barote, and E. U. Masumdar. Photoelectrochemical properties of spray deposited n-CdSe thin films. Solar Energy. 2010; 8: 763.
DOI:
https://doi.org/10.1016/j.solener.2010.01.026
43. Zhang, H., D. Yang, and X. Ma, 2007. Synthesis of flower-like CdS nanostructures by organic-free hydrothermal process and their optical properties. Materials Letters, 61(16), 3507-3510
https://doi.org/10.1016/j.matlet.2006.11.105.
44. Zhang, Y., F. Zhang, H. Wang, L. Wang, F. Wang, Q. Lin, and L. S. Li, 2019. High-efficiency CdSe/CdS nanorod–based red light–emitting diodes. Optics express, 27(6), 7935-7944.
DOI: https://doi.org/10.1364/OE.27.007935
45. Zhuang, X., Y. Ouyang, X. Wang, and A. Pan, 2019. Multicolor semiconductor lasers. Advanced Optical Materials, 7(17), 1900071.
DOI: https://doi.org/10.1002/adom.201900071